EFFECT OF NEGATIVE PRESSURE DIFFERENCE IRRIGATION ON SOIL WETTING PATTERN

EFFET D'UNE IRRIGATION SOUS DIFFÉRENCE DE PRESSION NÉGATIVE SUR LE SOL MOUILLANT MOTIF

S. M. Moniruzzaman[1], Teruyuki Fukuhara[2], Yoshihiro ISHII[3] and Hiroaki Terasaki[4]

ABSTRACT

Negative pressure difference irrigation (NPDI) is considered to be a highly efficient water saving method, which consists of a porous pipe and a water reservoir. The water use efficiency of the NPDI is higher than that of other irrigation methods such as surface irrigation, sprinkler irrigation and drip irrigation. In order to investigate the effect of negative pressure difference on the soil wetting pattern and water balance of the NPDI, laboratory experiments were carried out using a soil column in a temperature and humidity controlled room. The supplied water (M_{sup}), soil water storage (M_{soil}), evaporation (M_{eva}), wetted soil surface area and configuration of wetted soil around the porous pipe were measured for three different negative pressures. Empirical equations were proposed for the calculation of wetted soil volume, M_{soil} , M_{eva} and M_{sup}.

The proposed simple methodology could well reproduce the temporal variations in the wetted soil volume, water use efficiency, M_{soil}, M_{eva} and M_{sup}.

RÉSUMÉ ET CONCLUSIONS

Le manque d'eau est une contrainte majeure dans le domaine de l'agriculture en milieux arides et semi-arides. Le système d'irrigation sous différence de pression négative (NPDI) pourrait être un des meilleurs moyens pour économiser cette eau étant donner qu'il dirige l'eau directement vers la racine de la zone visée. Le système NPDI est composé d'un tuyau poreux enterré verticalement dans un sol, un conduit d'alimentation en eau et un réservoir d'eau. Le réservoir est placé à une hauteur inférieure à celle du tuyau poreux de manière à obtenir une différence de pression négative, notée P_n, dans le tuyau poreux. Lorsque le potentiel matriciel, noté ψ, du sol environnant est inférieur à la pression P_n, l'eau va alors se déplacer du réservoir vers le tuyau poreux et s'écouler dans le sol environnant. Au contraire, lorsque ψ est supérieur à P_n, l'écoulement s'arrête automatiquement sans aucune opération manuelle. La différence de pression entre ψ et P_n est le moteur de l'eau conduite par

1- PhD Scholar, Environmental Heat and Hydraulics Laboratory, Department of Architecture and Civil Engineering, University of Fukui, 3-9-1 Bunkyo, Fukui 910-8507, Japan; Telephone: 81-776278595, Fax: 81-776278746, E-mail: monir92us@yahoo.com

2- Dr. of Eng., Professor, Environmental Heat and Hydraulics Laboratory, Department of Architecture and Civil Engineering, University of Fukui, 3-9-1 Bunkyo, Fukui 910-8507, Japan; Telephone: 81-776278595, Fax: 81-776278746, E-mail: fukuhara@u-fukui.ac.jp

3- Dr. of Eng., Associate Professor, Dept. of Civil Engineering and Urban Design, Hiroshima Institute of Technology, 2-1-1 Miyake, Saeki-ku, Hiroshima 731-5193, Japan; E-mail: ishii@ycc.it.hiroshima.ac.jp

4- PhD Student, Environmental Heat and Hydraulics Laboratory, Department of Architecture and Civil Engineering, University of Fukui, 3-9-1 Bunkyo, Fukui 910-8507, Japan

le système NPDI. La présence d'un sol humide autour du tuyau poreux affecte l'efficacité de l'eau utilisée dans le domaine agricole. C'est pourquoi, il est important de comprendre la relation entre la configuration du sol mouillé et P_n au fil du temps l'approvisionnement en eau.
Ce document vise, dans un premier temps, à décrire l'influence d'une différence de pression négative sur un sol humide autour d'un tuyau poreux, et, dans un second temps, à prédire une méthode simple d'équilibre de l'eau au sein du système NPDI.
En vue d'atteindre l'objectif ci-dessus, un test d'équilibre de l'eau du système NPDI a été réalisée à une température et humidité ambiante contrôlée (25°C et 30%, respectivement) pour trois différents P_n (-0,02 m, -0,07 m et - 0,10 m H_2O).Une colonne de terre (diamètre = 0,20 m et hauteur = 0,21 m) a été remplie avec du sable Kawanishi, celui-ci ayant une densité à sec de 1410 kg/m3. Un tuyau poreux (longueur = 0,1 m, rayon extérieur = 12,5 mm et épaisseur = 6 mm) a été enterré verticalement au centre de la colonne de terre. P_n représente la différence de hauteur entre la surface de l'eau dans le réservoir et le milieu du tuyau poreux, comme le montre la Figure 2. Deux balances électriques (pesée minimum = 100 mg) ont été utilisées pour mesurer simultanément la masse d'eau cumulée dans le réservoir, notée M_{sup} et la masse d'eau cumulée dans le sol, notée M_{soil}. Par différence (M_{sup} – M_{soil}), l'évaporation cumulée peut alors être déterminée, celle-ci étant noté M_{eva}.
Enfin, la terre sèche a été séparée de la colonne de terre dans le but d'évaluer la configuration de la terre humide à t = 24 h, t = 48 h et t = 72 h.
Les principales conclusions tirées de cette étude sont les suivantes :

(1) Précision de mesure des M_{sup} et M_{soil} a été assurée par le résultat, M_{sup} = M_{soil}, obtenu à partir d'un test d'équilibre de l'eau. Dans cet essai, l'équilibre de l'eau, l'évaporation n'a pas été autorisée à partir de la surface du sol.
(2) L'équation empirique pourrait concorder avec les résultats expérimentaux concernant la variation du temps au sein de M_{sup}, M_{soil} et M_{eva}, ainsi qu'avec l'expansion du temps d'humidité du sol.
(3) L'efficacité de l'utilisation de l'eau (=M_{soil} / M_{sup}) est comprise entre 1 et 0,92. De plus, l'efficacité accroit lorsque P_n diminue.
(4) Cette méthode est efficace pour l'évaluation de l'équilibre de l'eau du système NPDI.

1. INTRODUCTION

Water loss due to evaporation, deep percolation below the root zone and conveyance of water from the source to the agricultural field cannot be avoided in irrigation systems. In a sprinkler irrigation system, spray losses can become as high as 45% under extreme weather conditions such as bright sunlight, high temperature and low humidity (Frost and Schwalen, 1955). Irrigation techniques that help save water are indispensable to regions and countries with limited water resources and severe external evaporation conditions. The water wasted in the NPDI is less than that of the drip irrigation (Yabe et al., 1986). NPDI system is a kind of subsurface irrigation and is composed of a water reservoir and a porous pipe installed in soil. The water reservoir is placed at a lower elevation than the porous pipe to generate negative pressure, P_n. NPDI system may be divided into two categories according to the installation direction of the porous pipe, i.e. horizontal and vertical installation.
Most of the past studies on NPDI (For example, Kato et al., 1982, Tanigawa et al., 1988, Ashrafi et al., 2002 and Siyal et al., 2009) were dealt with soil wetting pattern around a porous pipe installed horizontally in soil. On the other hand, the soil wetting pattern around a vertically installed porous pipe has been hardly investigated except two groups of researchers (Peifu et al., 2004 and Akhoond et al., 2008). It can be easily expected that the soil wetting pattern will be different for vertically installed porous pipe from that of horizontally installed porous pipe. Since the configuration of the wetting front affects evaporation from the soil surface, it is important to examine the effects of the negative pressure on the temporal expansion of the wetting front.

Besides that, intelligent operation and management of any subsurface irrigation technique, including NPDI, would depend on the water balance in the irrigation system and the water use efficiency. The water balance has been, however, not discussed in the past studies. Therefore, an experimental study is essential to develop a simple methodology for predicting soil wetting pattern and the water balance in a NPDI system with a vertically installed porous pipe.

2. MECHANISM OF A NPDI SYSTEM

In the NPDI system, water moves in a water supply conduit that links a water reservoir and a porous pipe installed vertically in the soil as shown in Figure 1. When the soil water matric potential (hereafter referred to as matric potential), ψ, is smaller than the negative pressure in the porous pipe, P_n, water moves up from the water reservoir to the porous pipe and then percolates through the porous pipe into the surrounding soil. On the contrary, when ψ is equal to or larger than P_n, the seepage stops automatically without any artificial work. The supplied water per unit time (supplied water rate) is in proportion to the negative pressure difference (NPD), $|\psi - P_n|$. Saving water can be enhanced by the NPD because the supplied water rate, which is in proportion to the NPD, lessens or becomes zero automatically as the wetting process of the soil progresses.

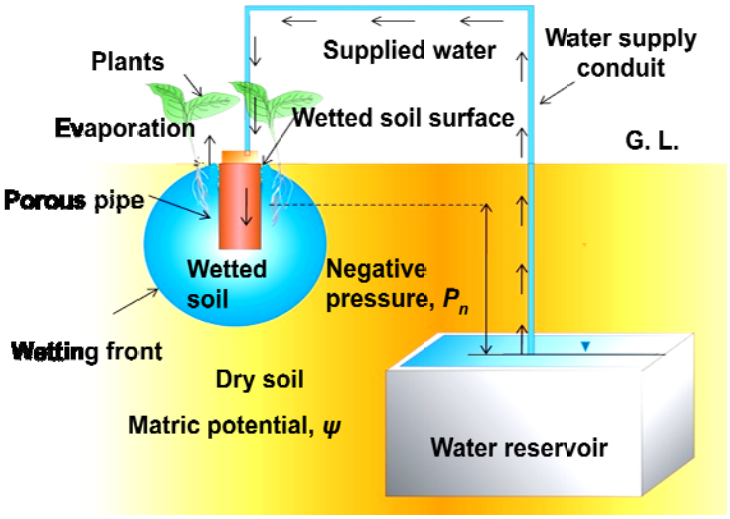

Figure 1. Mechanism of a negative pressure difference irrigation system (Mécanisme du système d'irrigation par différence de pression négative)

3. EXPERIMENTAL PROCEDURE

Figure 2 shows a schematic diagram of the experimental arrangement in a temperature and humidity controlled room (25°C and 30%, respectively). A Polyvinyl chloride pipe (diameter = 0.20 m and height = 0.21 m) was composed of seven rings with a height of 0.03 m each and used as a soil column. The soil column was filled with Kawanishi sand with a bulk density of 1410 kg/m^3 for all experimental cases. A porous pipe (length, l = 0.1 m, outer radius, R_p = 12.5 mm and thickness, t_p = 6 mm) was installed vertically in the center of the soil column as shown in Figure 2. A Marriott tube in a water supply tank was used to keep P_n constant. P_n was defined as the difference in elevation between the water surface in the reservoir (a-a) and intermediate elevation of the porous pipe (b-b) (see Figure 2).

Water was circulated between the porous pipe and the reservoir by using a small pump to remove air bubbles in the silicon tube. Two electric balances with a minimum reading of 0.1 g were placed under the soil column and under the reservoir and water supply tank, respectively. The electric balance placed under the soil column was used to measure the amount of water stored in the soil, M_{soil} (soil water storage, SWS), and the other balance was used to measure the amount of water supplied from the reservoir (supplied water), M_{sup}, simultaneously. All data were recorded at 60-minute intervals. Evaporation from the soil surface, M_{eva}, was given by subtracting M_{soil} from M_{sup}:

$$M_{eva} = M_{sup} - M_{soil} \tag{1}$$

For easy evaluation of the measurement accuracy of M_{sup} and M_{soil}, the soil column was wrapped so that evaporation from the soil surface was prevented (measurement accuracy test). Consequently, the measurement accuracy was evaluated for the simple water balance of $M_{sup} = M_{soil}$. After this measurement accuracy was secured, the water balance test was carried out for three different negative pressures (P_n = - 0.02, - 0.07 and - 0.1m H_20).

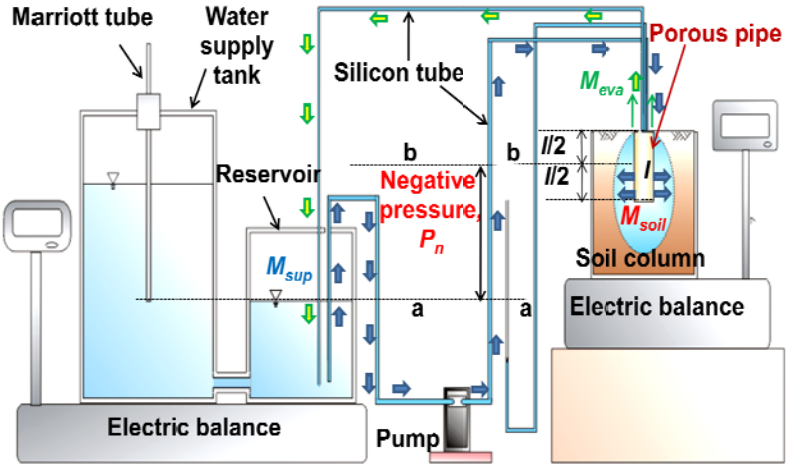

Figure 2. A Schematic diagram of a water balance test
(Schéma du test d'équilibre de l'eau)

After measuring M_{sup} and M_{soil} at the end of the test, dry soil around the wetted soil was removed from the soil column while taking off seven rings one at a time (see a photograph in Figure 4). Subsequently, the configuration of the wetting front was visualized and measured with a camera and a scale, respectively. Finally, the wetted soil was collected in a heat -proof tray and the volumetric water content of the wetted soil, θ_m, was obtained by the gravimetric soil sampling method. All data except M_{sup} and M_{soil} were measured at three elapsed time, t = 24, 48 and 72 hours.

4. RESULTS AND DISCUSSIONS

4.1 Measurement accuracy

Figure 3 shows the temporal variations in M_{sup} (> 0) and M_{soil} (< 0) for the measurement accuracy test for P_n = - 0.02 m. The difference between M_{sup} and M_{soil}, i.e. the measurement error (= $|M_{sup}-M_{soil}|/M_{sup}$) was negligibly small (1.4% or less) during the course of the experiment.

4.2 Soil wetting pattern

Figure 4 shows the observed wetting front at t =24 hours for P_n = - 0.02, - 0.07 and - 0.10 m, respectively.

A small photograph in Figure 4 shows the wetted soil around the porous pipe for P_n = - 0.02 m at t = 24 hours. The configuration of the wetted soil is circular in the horizontal plane. However, in the vertical plane, the configuration of the wetted soil is assumed to be similar to a truncated ellipsoid. Consequently, a simple approach is proposed for calculating the wetted soil volume, V_{wet}.

The volume of a truncated ellipsoid is given according to Acar et al., 2009:

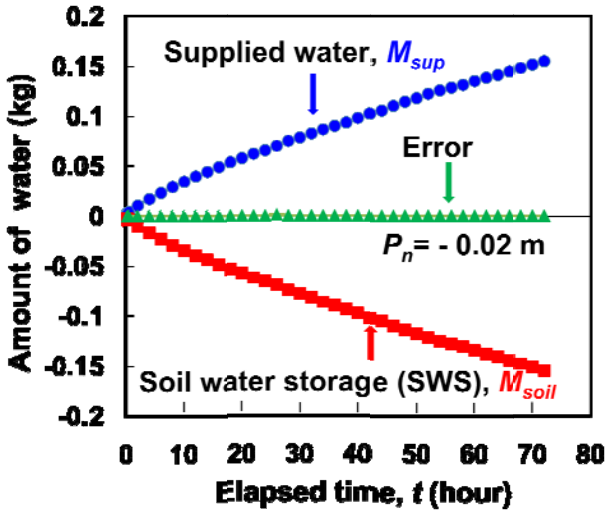

Figure 3. Water balance in measurement accuracy test
(L'équilibre de l'eau dans l'essai d'exactitude de mesure)

$$\frac{r^2}{R_m{}^2} + \frac{(z+H)^2}{B^2} = 1 \tag{2}$$

where r is the radial coordinate, z is the vertical coordinate (z = 0 : the soil surface), R_m is the maximum radial spread of the wetting front , H is the value of z corresponding to R_m and B is the distance between the maximum vertical spread of the wetting front and the vertical coordinate of R_m . The representative lengths of the wetting front (H, R_m and B) are defined in Figure 4. H, R_m and B are called geometric parameters. The truncated ellipsoid volume, V_t, is derived from the following integration:

$$V_t = \pi \int_{-B-H}^{0} r^2(z)\,dz \tag{3}$$

After substituting Eq. (2) into Eq. (3), V_{wet} is obtained by subtracting the volume of the porous pipe from V_t and is given by the following equation:

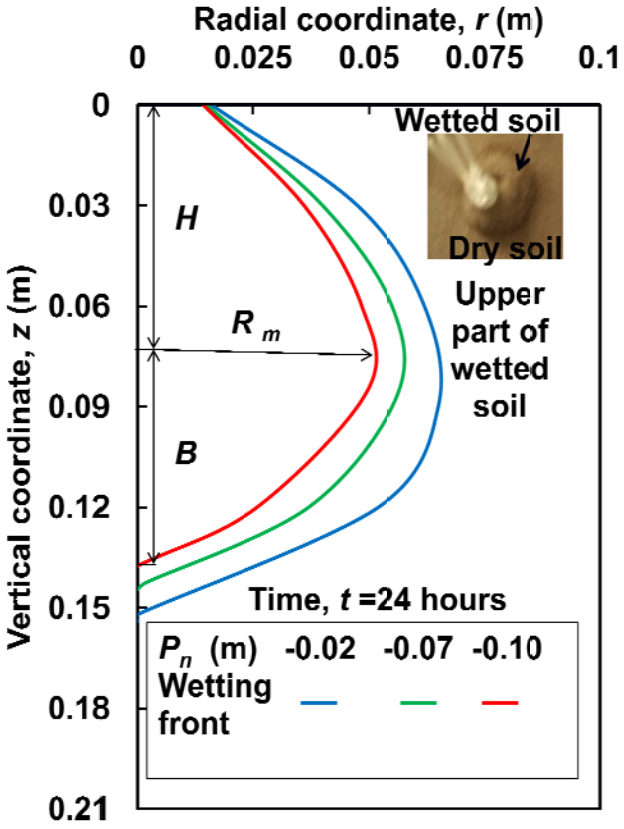

Figure 4. Wetting front in vertical plane for different negative pressures (Front de mouillage dans le plan vertical pour différentes pressions négatives)

$$V_{wet} = V_t - \pi R_p^2 l = \frac{R_m{}^2 \pi}{3B^2}(B+H)^2 \times (2B-H) - \pi R_p{}^2 l \tag{4}$$

Figure 5 shows the comparison between the calculated V_{wet} and the observed one. The former was obtained by substituting B, H and R_m measured in Eq. (4). The latter was obtained from the configuration of the wetting front, measured from the photographs and with a ruler. It is seen that the wetted soil can be considered as a truncated ellipsoid as long as Kawanishi sand is used. Since the wetting front is expanded with the decrease in $|P_n|$ at the same t (see Figure 4), we examined the relation of P_n to the temporal variations in H, R_m and B.

Figure 6 shows the expansion of the wetting front, i.e. the temporal increase in the geometric parameters associated with the change in P_n (for P_n = - 0.02, - 0.07 and - 0.10 m). Solid lines in Figure 6 express Eqs. (5), (6) and (7) for 24 ≤ t ≤ 72 hours.

$$H = pt^q \tag{5}$$

$$R_m = it^j \tag{6}$$

$$B = mt^n \tag{7}$$

where q = 0.05, j = 0.14, n = 0.14 and

$$p = 0.07P_n + 0.08 \quad (8)$$

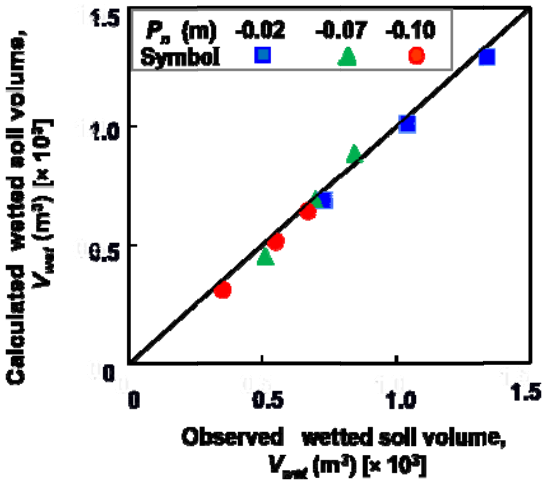

Figure 5. Accuracy of wetted soil volume (Précision du volume de sol mouillé)

$$i = 0.10P_n + 0.04 \quad (9)$$

$$m = 0.06P_n + 0.04 \quad (10)$$

The relation between each of the geometric parameters and t has a similarity, regardless of P_n as long as Kawanishi sand is used.
Figure 7 shows the comparison of the temporal variations in the calculated and observed V_{wet}. V_{wet} was calculated by substituting Eqs. (5) through (10) into Eq. (4). It is seen that Eq. (4) is applicable to predict the value of V_{wet}.

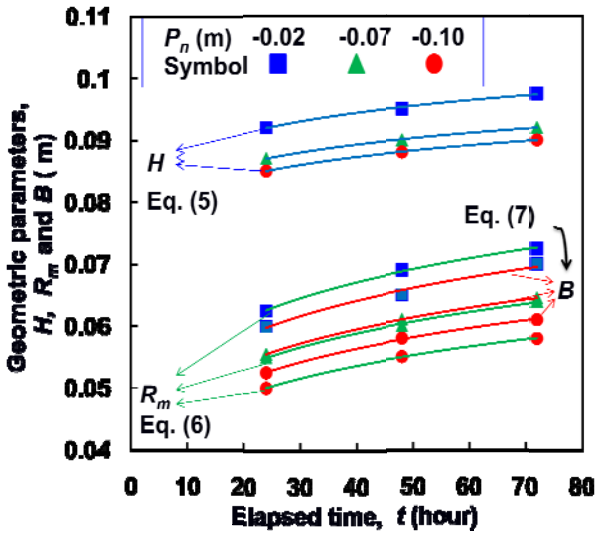

Figure 6. Temporal variations in geometric parameters, H, R_m and B (Les variations temporelles des paramètres géométriques, H, R_m et B)

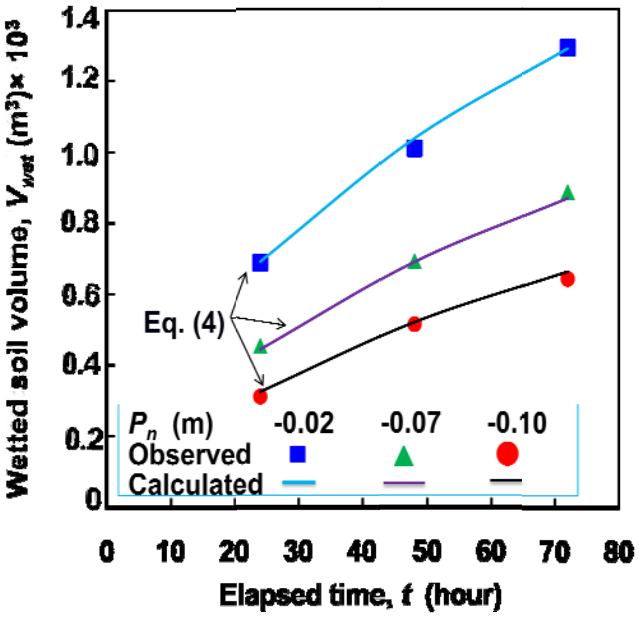

Figure 7. Comparison of observed and calculated temporal variations in wetted soil volume (Comparaison des valeurs observées et calculées des variations temporelles du volume de sol mouillé)

4.3 Soil water storage

Figure 8 shows the temporal variations in the volumetric water content, θ_m, for every P_n. The time gradient of θ_m, $d\theta_m/dt$, is very small for $t \leq 72$ hours but tends to increase with a decrease in $|P_n|$.

Time dependency of θ_m for each P_n can be expressed by (for $24 \leq t \leq 72$ hours):

$$\theta_m = ut^s \tag{11}$$

In Eq. (11), the co-efficients, s and u are given in terms of P_n as follows:

$$s = 0.08P_n + 0.09 \tag{12}$$

$$u = -4.35P_n^{\,2} - 0.11P_n + 0.07 \tag{13}$$

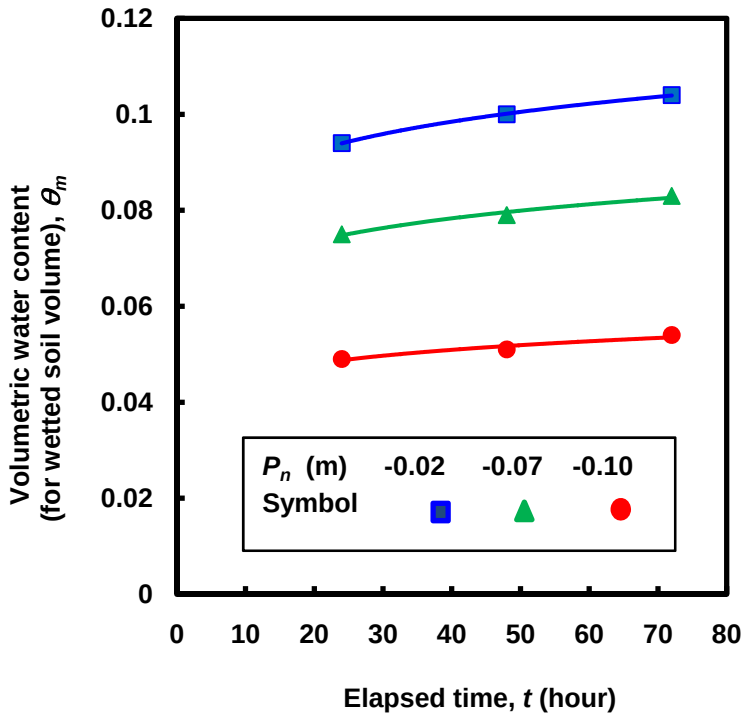

Figure 8. Temporal variations in volumetric water content
(Les variations temporelles de la teneur en eau volumétrique)

Finally, M_{soil} is calculated by the following equation:

$$M_{soil} = \rho_w \theta_m V_{wet} \tag{14}$$

where ρ_w is the density of water.

Figure 9 shows the observed M_{soil} obtained from the electric balance reading and M_{soil} calculated by substistuting Eqs. (4) and (11) into Eq. (14). Initially, M_{soil} increased remarkably with t and then the time increment of M_{soil} gradually became small. Both the observed and calculated M_{soil} are in good agreement with each other.

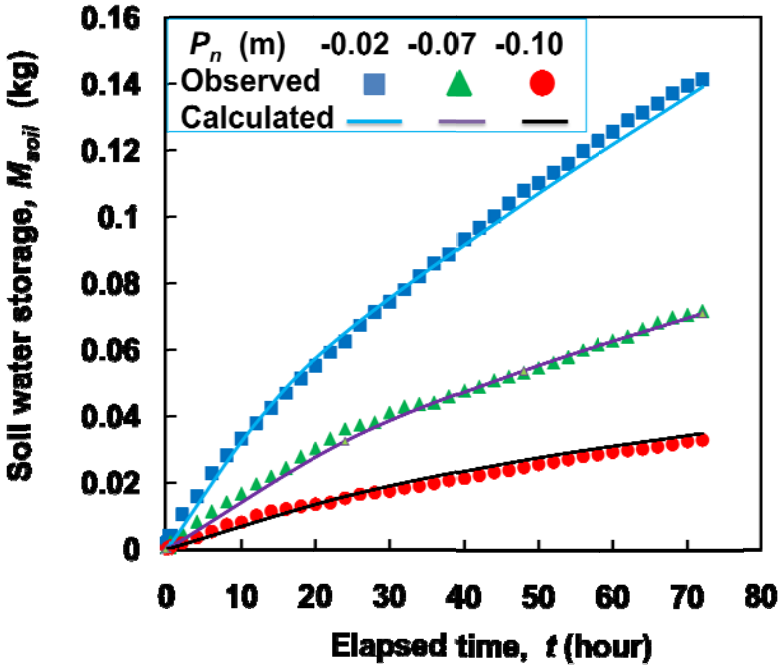

Figure 9. Comparison of observed and calculated temporal variations in soil water storage (Comparaison des valeurs observées et calculées les variations temporelles de stockage de l'eau du sol)

4.4 Evaporation

Figure 10 shows the relation between the wetted soil surface area, A_{wet}, around the porous pipe and t. A_{wet} increased with a decrease in $|P_n|$ at the same t. The temporal variation in A_{wet} is described by the following linear equation for every P_n for $24 \le t \le 72$ hours:

$$A_{wet} = c_1 t + d \tag{15}$$

where $c_1 = 1 \times 10^{-6}$ and

$$d = 0.0003 + 0.0005 P_n - 0.0167 P_n^{\,2} \tag{16}$$

Figure 11 shows the relation between evaporation rate, M_{heva} and A_{wet}. M_{heva} has a linear relation to A_{wet} approximately, regardless of P_n. The gradient of M_{heva}, i.e. dM_{heva}/dA_{wet} means the evaporation mass flux, m_{heva}. The value of m_{heva} becomes small with the increase in $|P_n|$ and is given by the following equation:

$$m_{heva} = 4.58 P_n + 0.58 \tag{17}$$

When the soil surface is wet, the evaporation rate, M_{heva}, can be calculated by the following equation:

$$M_{heva} = m_{heva} A_{wet} \tag{18}$$

In order to calculate the temporal variation in M_{eva}, the following assumptions were made in this study.

1. Evaporation from the soil surface begins simultaneously with the appearance of the wetted soil surface.
2. The appearance time of the wetted soil surface is the same as the commencement time of evaporation, t_i.

The values of t_i observed were 4, 8 and 16 hours for P_n = - 0.02, - 0.07and - 0.10 m, respectively.

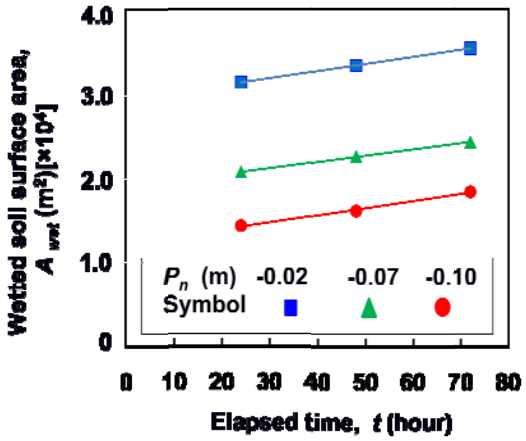

Figure 10. Temporal variations in wetted soil surface area (Les variations temporelles dans le sol mouillé surface)

Figure 12 illustrates the decision procedure of M_{soil} required for the appearance of the wetted soil surface, i.e. M_c according to the above assumptions. M_{c1}, M_{c2} and M_{c3} in Figure 12 correspond to M_c at observed t_i for P_n = - 0.02, - 0.07 and - 0.1 m, respectively. Since the deviations between M_{c1}, M_{c2} and M_{c3} were small, the mean of these three values [= (M_{c1}+M_{c2}+M_{c3})/3] was adopted as M_c (= 0.014 kg). As a result, the calculation of M_{eva} was started at time (t = t_{ic}) when M_{soil} reached M_c. M_c is called the critical SWS in this paper.

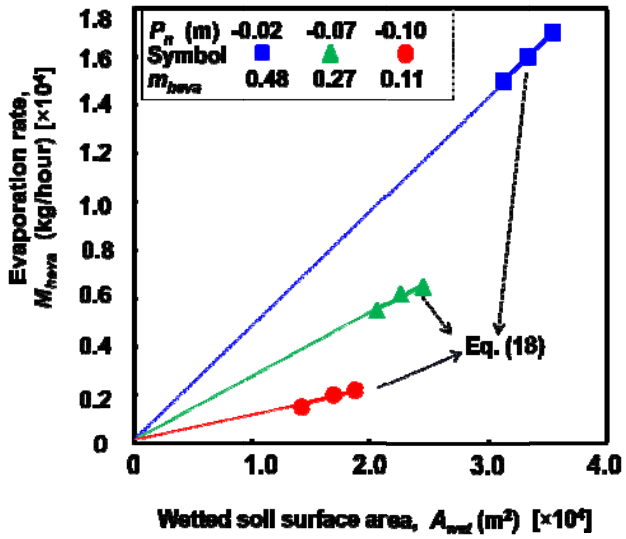

Figure 11. Relation between evaporation rate and wetted soil surface area (Relation entre le taux d'évaporation et la surface de sol humide)

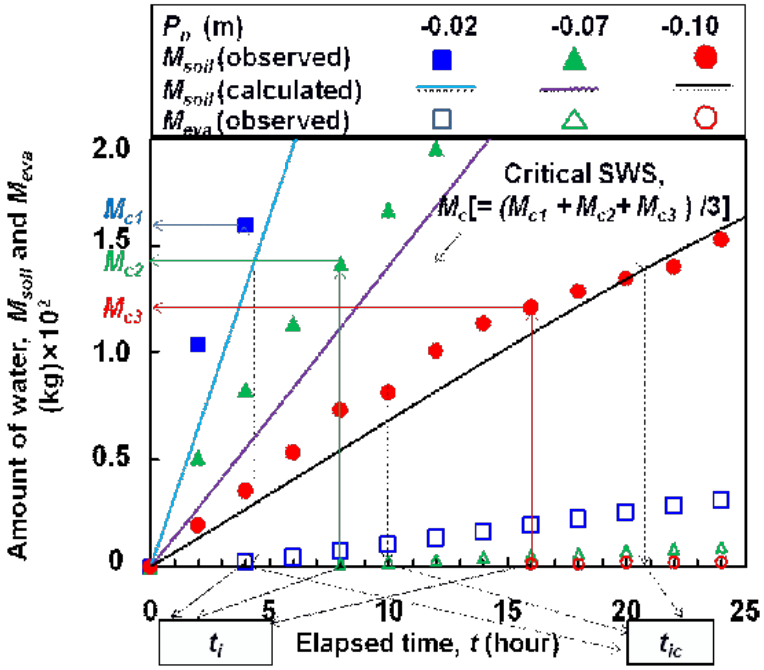

Figure 12. Decision procedure of critical soil water storage (Procédure de décision de stockage en eau du sol critiques)

Figure 13 shows the comparision of the observed M_{eva} and calculated one. After substituting Eqs. (15) and (17) into Eq. (18), M_{eva} was calculated by the following equation:

$$M_{eva} = \int_{t_{ic}}^{t} M_{heva}\, dt \tag{19}$$

It is seen that there is little discrepancy between the calculated M_{eva} and the observed one for every P_n even though the maximum difference between t_i and t_{ic} was about 5 hours (see Figure 12).

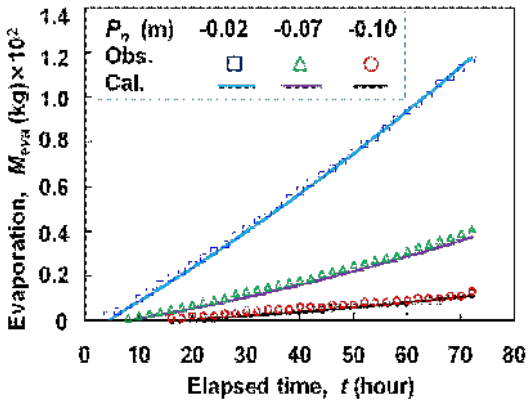

Figure 13. Comparison of observed and calculated temporal variations in evaporation (Comparaison des valeurs observées et calculées les variations temporelles de l'évaporation)

4.5 Supplied water

Figure 14 shows the observed M_{sup} obtained from the electric balance reading and M_{sup} calculated by substistuting Eqs. (14) and (19) into Eq. (1). Initially, M_{sup} increased remarkably with t and then the time increment of M_{sup} gradually became small. Both the observed M_{sup} and the calculated one show good agreement.

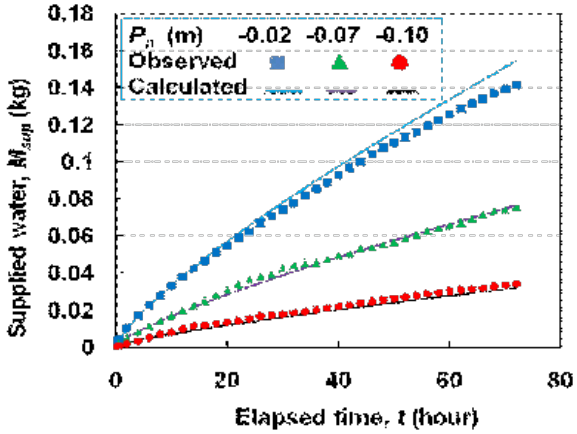

Figure 14. Comparison of observed and calculated temporal variations in supplied water (Comparaison des valeurs observées et calculées les variations temporelles de l'eau fournie)

4.6 Water use efficiency

The water use efficiency, E_f, is defined as the ratio of M_{soil} to M_{sup}, i.e. M_{soil} / M_{sup}. The calculated water use efficiency was obtained by using Eqs. (1), (14) and (19). Figure 15 shows the comparison of the observed E_f and the calculated one for different P_n. E_f decreased remarkably with t at the commencement of evaporation and then decreased gradually. E_f ranged from 1.0 to 0.92 at different P_n. The calculated E_f - t relation agreed with observed one for every P_n.

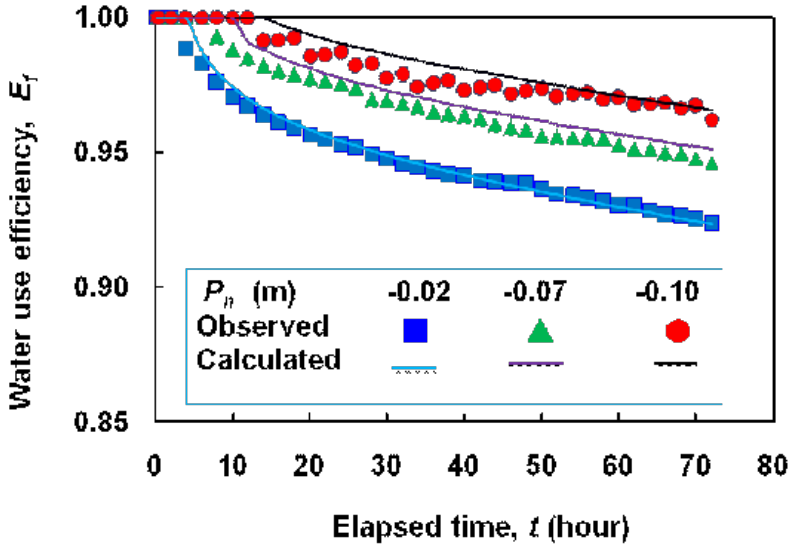

Figure 15. Comparison of observed and calculated temporal variations in water use efficiency (Comparaison des valeurs observées et calculées des variations temporelles l'efficience d'utilisation de l'eau)

5. CONCLUSIONS

For investigating the soil wetting pattern and water balance in the negative pressure difference irrigation (NPDI) system, a laboratory experiment was performed using a soil column, a porous pipe vertically installed in soil and a water reservoir under conditions of constant air temperature and humidity. The supplied water, soil water storage, evaporation, wetted soil surface area and configuration of wetted soil around the porous pipe were measured for three different negative pressures, -0.02, -0.07 and -0.1 m.

The main conclusions drawn from the present study are as follows:

1) The wetted soil can be considered as a truncated ellipsoid as long as Kawanishi sand is used.
2) The proposed empirical model can well reproduce the temporal variations in the wetted soil volume, soil water storage, evaporation and supplied water.
3) The commencement time of evaporation is delayed as the negative water pressure decreases.
4) With a decrease in the negative pressure, the water use efficiency increases and is above 92% in all the cases.

6. REFERENCES

1. Acar, B., Topak, R., and Mikailsoy, F., 2009. Effect of applied water and discharge rate on wetted soil volume in loam or clay-loam soil from an irrigated trickle source. African J. of Agric. Res., 4(1):49 - 54.
2. Akhoond, A. M. and Golabi, M., 2008. Subsurface porous pipe irrigation with vertical option as a suitable irrigation method for light soils. Asian J. of Scientific Research, 1(3):180-192.
3. Ashrafi, S., Gupta, A. D., Babel, M. S., Izumi, N. and Loof, R., 2002. Simulation of infiltration from porous clay pipe in subsurface irrigation. Hydrological Sciences-Journal, 47(2):253-268.
4. Frost, K. R. and Schwalen, H. C., 1955. Sprinkler evaporation losses. Agric. Eng., 36(8): 526 - 528.
5. Kato, Z., and Tejima, S., 1982. Theory and fundamental studies on subsurface irrigation method by use of negative pressure. Trans. JSIDRE, 101:46-54.
6. Peifu, J., Lei, T., Xiao, J., Yu, Y. and Bralts, V. F., 2004. A new irrigation system of zero/ negative pressure and the experimental verification of its feasibility. ASAE/CSAE Annual International Meeting Presentation, paper no. 042253, Ontario, Canada.
7. Siyal, A. A. and Skaggs, T. H., 2009. Measured and simulated soil wetting patterns under porous clay pipe sub-surface irrigation. J. of Agricultural Water Management, 96:893-904.
8. Tanigawa, T., Yabe, K. and Tejima, S., 1988. Comparison of prediction of actual measurement about dynamic distribution of soil moisture tension. Trans. JSIDRE, 137:9-16.
9. Yabe, K., Kato, Z. and Tejima, S., 1986. Disparities of water management in the sub-irrigation method by negative pressure difference and the drip irrigation method. Trans. JSIDRE, 123:11-16.